Solvent Exclusion and Chemical Contrast in Scanning Force Microscopy

S. K. Sinniah,[†] A. B. Steel, C. J. Miller, and J. E. Reutt-Robey*

Contribution from the Department of Chemistry and Biochemistry, Calvin College,
Grand Rapids, Michigan 49546, and Department of Chemistry and Biochemistry,
University of Maryland, College Park, Maryland 20742

Received April 19, 1996[⊗]

Abstract: The importance of a solvent in regulating the adhesion forces between surfaces is studied quantitatively with scanning force microscopy. Both samples and tips are coated with alkyl thiolate monolayers of type $HS(CH_2)_{10}Y$ and force measurements are conducted as a function of terminal group Y (Y = CH_2CH_3, CH_2OCH_3, CO_2CH_3, $CO(NH_2)$, CO_2H, and CH_2OH) and solvent (water, ethanol, and *n*-hexadecane). Adhesive forces in water span the greatest range (0.30−12.5 nN), with hydrophobic surfaces adhering most strongly and hydrophilic surfaces most weakly. In ethanol the adhesive forces are substantially smaller and in *n*-hexadecane they are negligible. In water, these adhesive forces are consistent with the work required to exclude solvent from the tip−sample interface, indicating that solvent exclusion dominates adhesion. Such macroscopic solvent exclusion cannot fully explain the adhesive forces in ethanol. This force data is used to evaluate the tip−sample interfacial energies (γ_{ts}) of like CH_3- and CH_2OCH_3-terminated surfaces and the surface−vacuum interfacial energies (γ_{sv}) of the hydrophilic surfaces. An effective tip radius of ∼30 nm and contact area of ∼10 nm^2 (or ∼50 contacting molecules) is estimated from the adhesion between methyl groups in water. Since solvent exclusion regulates adhesion between these model organic surfaces, it provides a source of chemical contrast in force imaging. We explore this chemical contrast with friction force measurements of *co-block* polyethylene glycol−polyamide polymer surfaces.

Introduction

A new generation of scanning force microscopies (SFM), evolved from atomic force microscopy, is seeking to push the frontiers of force measurements beyond simple topography. Several groups have already demonstrated the ability to distinguish interactions between different tip−sample functional groups and to map out the spatial arrangement of these groups on patterned and phase−separated monolayer surfaces.[1−5] The “chemical contrast” obtained in these systems has been interpreted primarily in terms of chemical interactions between the monolayer coatings on the tip and samples. It is noted that tips without such monolayer coatings have successfully imaged and identified compositional domains of Langmuir−Blodgett films[6,7] and self-assembled monolayers.[8] Mechanical effects (i.e. variations in the surface compliance) will also contribute to the observed image contrast, as recently demonstrated in force measurements of mixed chain length monolayer films.[9]

The prospect of distinguishing chemical structure at the surface−liquid interface is of great interest but introduces the additional complication of the medium's role in regulating tip−sample interactions. While scanning force measurements under liquids have proliferated, we have found no systematic study relating the measured adhesive forces to the work of adhesion under liquids. This is unfortunate, as liquids are the preferred media to achieve true atomic resolution in force imaging, to investigate biological systems under relevant conditions, and to elucidate the compositional and structural sensitivity of surfaces to liquid contact. This paper explores the relationship between the measured adhesive forces and the thermodynamic work of adhesion in liquid media.

The work of adhesion, *w*, in a liquid medium includes solvent terms which, in the thermodynamic limit, are related to the force of adhesion, *F*:

$$F \propto w = (\gamma_{sl} + \gamma_{tl}) - \gamma_{ts} \qquad (1)$$

where γ_{sl} and γ_{tl} represent the sample−liquid and tip−liquid interfacial energies, respectively, and γ_{ts} is the tip−sample interfacial energy. We may think of both γ_{sl} and γ_{tl} terms combining to give the work due to solvent exclusion, i.e. $w_{se} = \gamma_{sl} + \gamma_{tl}$. Previous AFM measurements have shown that the adhesive forces vary dramatically with solvent, with ethanol proving optimal for force reduction,[10] In this paper we attempt to place these observations on a more quantitative footing by comparing measurements of adhesive forces to the thermodynamic work of adhesion. Our data set is generated from Au samples and Au-coated AFM tips, each coated with monolayer films of functionalized self-assembled alkanethiol monolayers ($HS(CH_2)_{10}Y$), where the Y terminations include CH_2CH_3, CH_2OCH_3, CO_2CH_3, $CO(NH_2)$, CO_2H, and CH_2OH, as shown schematically in Figure 1.[11] Data are reported for three

---

[†] Calvin College.

[⊗] Abstract published in *Advance ACS Abstracts*, September 1, 1996.

(1) Frisbie, C. D.; Rozsnyai, L. F.; Noy, A.; Wrighton, M. S.; Lieber, C. *Science* **1994**, *265*, 2071−2074.

(2) Noy, A.; Frisbie, C. D.; Rozsnyai, L. F.; Wrighton, M. S.; Lieber, C. M. *J. Am. Chem. Soc.* **1995**, *117*, 7943−7951.

(3) Green, J.-B. D.; McDermott, M. T.; Porter, M. D.; Siperko, L. M. *J. Phys. Chem.* **1995**, *99*, 10960−10965.

(4) Berger, C. E. H.; van der Werf, K. O.; Kooyman, R. P. H.; de Grooth, B. G.; and Greve, J. *Langmuir* **1995**, *11*, 4188−4192.

(5) Akari, S.; Schrepp, W.; Horn, D. *Langmuir* **1996**, 21, 857−860.

(6) Overney, R. M.; Meyer, E.; Frommer, J.; Guntherodt, H.-J.; Fujihara, M.; Takano, H.; Gotoh, Y. *Nature* **1992**, *359*, 133−135.

(7) Overney, R. M.; Meyer, E.; Frommer, J.; Guntherodt, H.-J.; Fujihara, M.; Takano, H.; Gotoh, Y. Langmuir **1994** *10*, 1281−1286.

(8) Wilbur, J. L.; Biebuyck, H. A.; MacDonald, J. C.; Whitesides, G. M. *Langmuir* **1995**, *11*, 825−831.

(9) Koleske, D. D.; Barger, W. R.; Lee, G. U.; Colton, R. J. *Langmuir* **1996**, in press.

(10) Weisenhorn, A. L.; Maivald, P.; Butt, H.-J.; Hansma, P. K. *Phys. Rev. B* **1992**, *45*, 11226−11232.

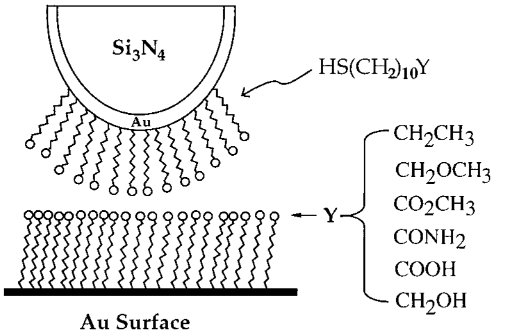

Figure 1. Schematic illustration of the tip and sample under adhesive contact. Sample and cantilever tip are coated with alkyl thiolate monolayers of type $HS(CH_2)_{10}Y$, with terminal groups Y as shown.

prototypical solvents—water, *n*-hexadecane (HD), and ethanol (EtOH). These systems were chosen because the methodology for sample and tip modification are well-known, and the tips/samples are robust under the liquids and the forces of our investigation. The comprehensive contact angle data base generated by Whitesides and co-workers for these systems and solvents[12−14] and appropriate thermodynamic relations allow us to evaluate key terms in eq 1, providing an essential basis for interpreting our force data. In water, we find that the force of adhesion scales directly to the work required to exclude solvent from the tip−sample interface. The contact area deduced from this relationship (∼10 nm^2 for contacting CH_3 groups in water) is also very reasonable. From this data we further estimate the interfacial tension between tip and sample, γ_{ts}, for like hydrophobic surfaces and the surface−vacuum interfacial energy, γ_{sv}, for hydrophilic surfaces. These results suggest guidelines to tip and solvent selection for enhancing chemical contrast in force measurements. This approach is demonstrated with an application involving a *co-block* polymer surface.

Experimental Section

Sample and Tip Fabrication. All the functionalized mercaptans were synthesized from the bromides via reaction with thiourea followed by NaOH, as described previously.[15] 1-Carbamoyl-11-bromoundecane, $Br(CH_2)_{10}CONH_2$, was obtained from the reaction of 1-bromoundecanoyl chloride with ammonia. Methyl 11-bromoundecanoate, $Br(CH_2)_{10}CO_2CH_3$, was synthesized from 11-bromoundecanoyl chloride with methanol. The bromoundecanoyl chloride was produced from the reaction of 11-bromoundecanoic acid with thionyl chloride. The 11-methoxy-1-bromoundecane, $Br(CH_2)_{11}OCH_3$, was obtained by the reaction of 11-bromo-1-undecanol with sodium hydride followed by the addition of methyl iodide. The final purification of the mercaptan was via flash chromatography on silica gel using mixtures of ethyl acetate and chloroform. Distilled, deionized water [18 MΩ cm resistivity from a MilliQ (Millipore) filtration system] was used for the force measurements. *n*-Hexadecane was purified by passing through activated alumina. The absolute ethanol (Pharmco) was used as received. All other chemicals were purchased from Aldrich and used as received.

Samples were prepared by depositing a *ca.* 500 Å Cr adhesion layer, followed by a *ca.* 4000 Å Au layer (each 99.99% purity) onto glass microscope slides by radio frequency (rf) sputtering. The microscope slides were subsequently cut into 5 mm × 5 mm substrates. These Au substrates were cleaned through successive exposures of chromic acid followed by 5% aqueous HF as described previously.[15] Adsorption of each functionalized alkyl mercaptan was conducted in a 20−50 mM solution of the corresponding mercaptan in 95% ethanol, and a minimum of 4 h in solution (more typically overnight) was allotted to film self-assembly. Contact angles for water on the substrates measured using a contact angle goniometer (Rame-Hart) matched the contact angle data of Whitesides and co-workers.[12−14] Functionalized AFM tips were prepared in a similar manner. Conventional Si_3N_4 AFM cantilevers with integrated tips (Digital Instruments) were first plasma-cleaned, Cr/Au coated (*ca.* 50 and 500 Å, respectively) by rf sputtering, and immediately immersed into the mercaptan solutions.

The polyethylene glycol-*block*-polyamide copolymer (tradename PEBAX 1074) was a gift from W. R. Grace & Co. and was manufactured by Elf Atochemical. Fresh surfaces with ∼40 nm root mean square roughness suitable for scanning force measurements were prepared by melting and resolidifying individual pellets.

Force Measurements. All force measurements were conducted with a Digital Instruments multimode microscope (Nanoscope III), utilizing a small liquid cell. The reproducibility of the adhesive pull-out measurements for a given tip (and the possibility of sample or tip damage) was monitored by successively measuring the pull-out forces for individual force−distance curves at several isolated points on the sample. For the majority of the functionalized tips, no significant change in pull-out force was observed for as many pull-out measurements (>50) as conducted at a given site, consistent with previous studies of the mechanical stability of alkyl thiolate monolayers under an applied load.[16] The few tips which failed to give reproducible force measurements were discarded. Having established the reliability of a tip, 50 force−distance curves typically were signal averaged at a single surface site to improve the statistics of the pull-out measurement. This process was repeated at a minimum of 10 random sites per sample. The precision of these force measurements is somewhat limited, with the standard deviation in the pull-out forces for a particular tip−sample pair falling at ∼10% of the average pull-out force value. Changing the tips and samples resulted in a broader distribution in the adhesive force values, with the standard deviation increasing to as much as 30% of the average pull-out value for a sampling of five distinct tip−sample sets. This limited reproducibility is attributed primarily to variations in the tip and sample structures, which led to variations in contact area. The adhesive force measurements that we report for tips and samples coated with chemically distinct monolayer coatings are averaged from a minimum of four distinct tip−sample combinations. For measurements between like self assembled monolayer surfaces, we typically utilized two to four distinct tip−sample combinations for each chemical termination. This limited sampling was adopted in the interest of performing measurements on a chemically diverse range of samples and tips.

In order to report absolute force values, the force constants of the tips were calibrated according to the method described by Sader *et al.*[17] This calibration requires knowledge of the cantilever mass and dimensions and a determination of the unloaded resonant frequency of the cantilever. This method has been tested and compared with the cantilever calibration method of Cleveland *et al.*,[18] in which the spring constant is determined by measuring the resonant frequency before and after the addition of small masses. In our calibration, care was taken to account for both damping in air and the gold coating on the cantilevers. Measurements were conducted with the nominally 200 and 100 μm length narrow-legged V-shaped cantilevers acquired from Digital Instruments and modified as above. Using this approach, we calibrated 48 cantilevers for each length and found very little variation among the cantilevers of a given length with respect to the resonant frequency. Table 1 summarizes the range of spring constants obtained for the 200 and 100 μm length modified cantilevers.

---

(11) Although we cannot exclude the mechanical component of the adhesive forces, we have utilized a series of chemically modified SAMS with the same nominal hydrocarbon chain length. Consequently, observed differences should primarily reflect the chemical differences in chain termination.

(12) Bain, C. D.; Whitesides, G. M. *Angew. Chem. Int. Ed. Engl.* **1989**, *28*, 506−512.

(13) Bain, C. D.; Troughton, E. B.; Tao, Y.-T.; Evall, J.; Whitesides, G. M.; Nuzzo, R. G. *J. Am. Chem. Soc.* **1989**, *111*, 321−335.

(14) Bain, C. D.; Evall, J.; Whitesides, G. M. *J. Am. Chem. Soc.* **1989**, 111, 7155−7164.

(15) Becka, A.; Miller, C. J. *J. Phys. Chem.* **1992**, *96*, 2657.

(16) Salmeron, M.; Liu, G.-y.; Ogletree, D. F. *Forces in Scanning Probe Methods*; H.-J. Guntherodt, *et al.*, Eds.; Kluwer Academic Publishers: Netherlands, 1995; 593−598.

(17) Sader, J. E.; Larson, I.; Mulvaney, P.; White, L. R. *Rev. Sci. Inst.* **1995**, 66, 3789−3798.

(18) Cleveland, J. P.; Manne, S.; Bocek, D.; Hansma, P. K. *Rev. Sci. Inst.* **1993**, *64*, 403−405.

Table 1. Range of Spring Constants and Cantilever Resonant Frequencies Determined for the Chemically Functionalized Narrow-Legged Cantilevers

cantilever length	number tested	k(N/m)	resonant frequency in air (kHz)
200 μm (Au-coated)	48	0.024−0.030	11.5−13.0
100 μm (Au-coated)	48	0.089−0.112	31.5−36.5

Imaging Measurements. Using this AFM setup for topographic imaging, we can routinely resolve aperiodic surface structures, such as crystallographic steps, which are separated *ca.* 100 Å. Under the conditions of force imaging, we thus deduce a contact area on the order of 100 Å. This setup (with uncoated cantilevers) has also been used to resolve the lattice of hard surfaces, such as the cleavage face of MgO. However, the molecular-level details of monolayer structure are not the subject of this study.

Adhesion Results

Like Samples and Tips. Solvent regulation of tip−sample interactions is easily demonstrated with force−distance measurements for samples and tips coated with the same self-assembled monolayers. As shown in Figure 2a, a methyl-terminated alkyl thiol tip brought into contact with a methyl-terminated alkyl thiol sample shows a strong force of adhesion in water (pull-out force, $F_{po} = 20.7$ nN), but a much weaker force in ethanol ($F_{po} = 3.0$ nN), and a negligible force in HD ($F_{po} < 0.1$ nN!). Samples and tips with other terminations exhibit similar variations, but on a smaller scale. As shown in Figure 2b, a COOH-terminated alkyl thiol tip brought into contact with a COOH-terminated alkyl thiol sample shows a weaker force of adhesion in water ($F_{po} = 4.4$ nN), which decreases in ethanol ($F_{po} = 0.3$ nN) and diminishes further in HD ($F_{po} = 0.1$ nN). Note that these values are the pull-out values observed in single pull-out measurements. A statistical summary with average pull-out force values for like samples and tips is provided in Table 2.

We first consider the pull-out force values observed in water, which exhibit the greatest range of values, lending themselves to more detailed interpretation. Ideally, we would like to compare the measured pull-out forces (F_{po}) directly to the work of adhesion (w) for the functionalized alkyl thiol-coated tips and samples, as per eq 1. This requires knowledge of the tip−sample interfacial energy terms, γ_{ts}, and the sample-solvent and tip-solvent interfacial energy terms, γ_{sl} and γ_{tl}. In principle, these latter two terms may be evaluated via Young's equation:[19]

$$\gamma_{sl} = \gamma_{sv} - \gamma_{lv} \cos \theta \tag{2}$$

where γ_{sv} denotes the interfacial tension between the sample and vacuum, γ_{lv} denotes the interfacial tension between the solvent and vacuum, and θ represents the contact angle between the liquid and solid sample surface. Values for γ_{lv} can be measured directly and are well-known for the solvents of these investigations at room temperature: γ_{lv}(water) = 72.8 mN/m, γ_{lv}(EtOH) = 22.5 mN/m, and γ_{lv}(HD) = 27.6 mN/m.[20] Values for θ are available for all the functionalized self assembled monolayers in all of the solvents used in this study and are summarized in Table 3. (We caution that Young's equation is accurate only for those liquid−solid interfaces which are in thermodynamic equilibrium. For liquid−solid interfaces with contact angles <10°, equilibrium may not be established and Young's equation is approximate.)

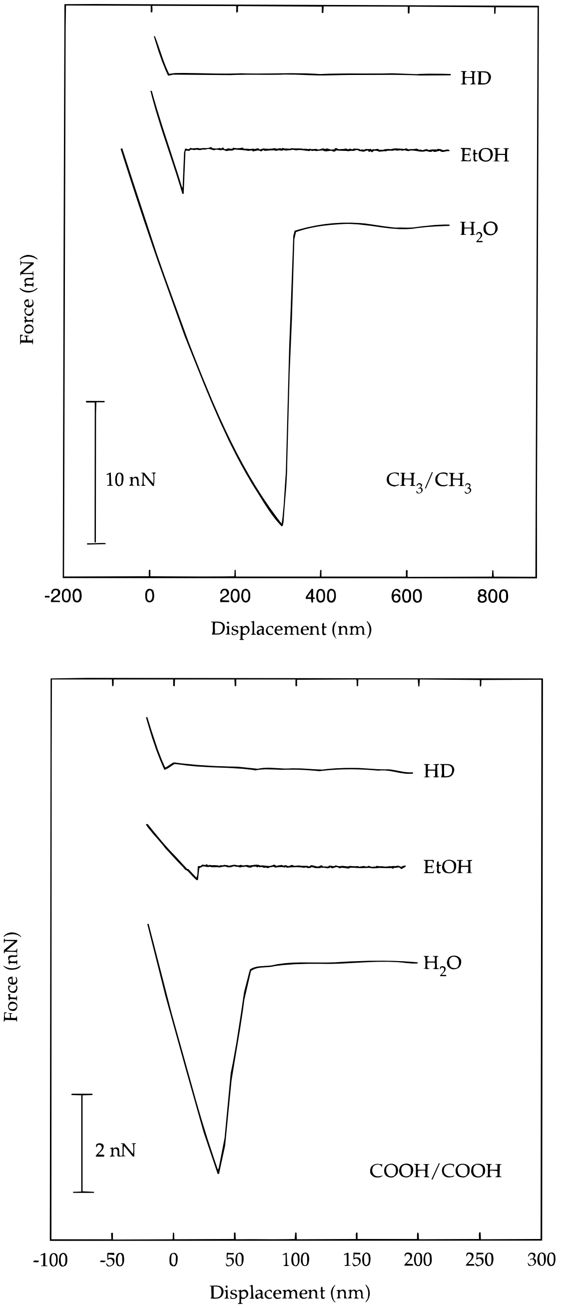

Figure 2. Representative force versus pull-out distance curves obtained in three solvents for alkyl thiolate covered samples and tips with same chemical terminations. Reported pull-out force values are the force difference between the adhesive minima and the separated (large displacement) values: (a) CH_3-terminated and (b) CO_2H-terminated.

For these like tip and sample monolayer coatings where γ_{ts} is very small (see below), the work may be expressed as

$$w \approx 2\gamma_{sl} = 2(\gamma_{sv} - \gamma_{lv} \cos \theta)$$

Although γ_{sv} values cannot be measured directly, they can be estimated for hydrophobic systems where the London dispersion interactions predominate (such as in HD), from the following generalization of Young's equation:[21]

$$\gamma_{sv} \text{ (or } \gamma_{tv}) = \gamma_{lv}(1 + \cos \theta)^2/4 \tag{3}$$

A value of 19.5 mN/m for γ_{sv} for the CH_3-terminated mono-

---

(19) Israelachvili, J. *Intermolecular and Surface Forces;* 2nd ed.; Academic Press Limited: San Diego, 1994.

(20) Jasper, J. J. *J. Phys. Chem. Ref. Data* **1972**, 1, 841.

(21) Chaudhury, M. K.; Whitesides, G. M. *Science* **1992**, *255*, 1230−1232.

Table 2. Summary of Pull-Out Forces *F* (nN) Recorded between Like Self-Assembled Monolayer Surfaces in Solvents

	solvent								
	water			EtOH			n-HD		
alkanethiol coating	N^a	F	$\sigma_F{}^b$	N^a	F	$\sigma_F{}^b$	N^a	F	$\sigma_F{}^b$
$HS(CH_2)_{10}CH_2CH_3$	4	12.5	4.4	6	2.3	1.1	4	0.07	0.05
$HS(CH_2)_{10}CH_2OCH_3$	3	5.3	0.6	3	0.31	0.04	2	0.62	0.43
$HS(CH_2)_{10}CO_2CH_3$	5	3.7	1.4	3	0.55	0.16	4	0.95	0.41
$HS(CH_2)_{10}CONH_2$	2	2.7	1.1	1	0.21	0.08	3	0.35	0.62
$HS(CH_2)_{10}CO_2H$	4	2.3	1.1	2	0.27	0.04	2	0.11	0.02
$HS(CH_2)_{10}CH_2OH$	4	0.30	0.05	2	0.18	0.18	8	1.27	1.20

[a] Number of independent tip/sample combinations used in the determination. $b\sigma_F$ denotes the standard deviation in the measurement of pull-out forces.

Table 3. Contact Angle Values between Like Self-Assembled Monolayer Surfaces in Solvents

	contact angle (deg)		
alkanethiol coating	water[a]	EtOH[b]	HD[a]
$HS(CH_2)_{10}CH_2CH_3$	112	40	47
$HS(CH_2)_{10}CH_2OCH_3$	75	<10	35
$HS(CH_2)_{10}CO_2CH_3$	67	<10	28
$HS(CH_2)_{10}CONH_2$	13	<10	<5
$HS(CH_2)_{10}CO_2H$	<10	<5	<5
$HS(CH_2)_{10}CH_2OH$	<10	<5	<5

[a] Reference 10. [b] Present study.

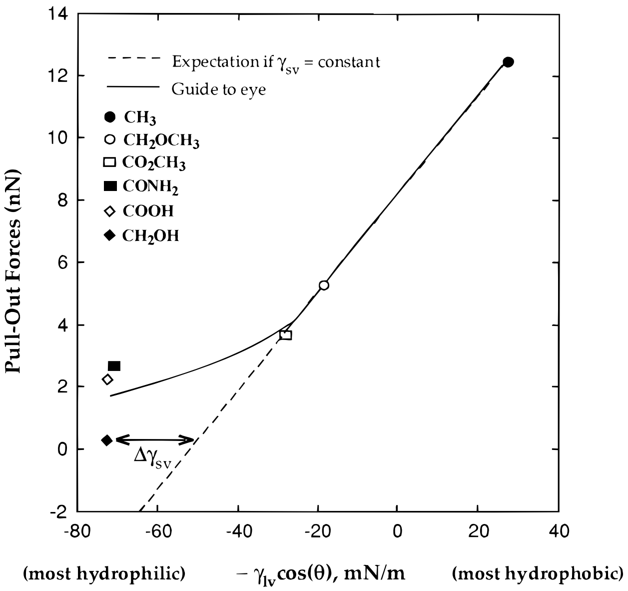

Figure 3. Adhesive pull-out forces (F_{po}) measured in water (points) versus $-\gamma_{lv}\cos\theta$. The solid line represents a guide to the eye. Variations in the adhesive forces are attributed to variations in the work (w) required to separate tip and sample surfaces in liquid water: $w \approx 2(\gamma_{sv} - \gamma_{lv}\cos\theta)$. The dashed line represents the force expected for constant γ_{sv}. Curvature is attributed to an increase in γ_{sv} for the acid monolayers above the 19.5 mN/m value known for the CH_3-terminated monolayers. Graphically, for the OH termination, the increase in surface energy is $\Delta\gamma_{sv} = 20$ mN/m. For the CO_2H and $CONH_2$ terminations, $\Delta\gamma_{sv} = 55$ mN/m.

layers can thus be determined. Since the other surface terminations employed in this study are polar and in some cases ionizable acids, eq 3 will underestimate the values for γ_{sv}. To assess the solvent contribution to the force of adhesion, we thus plot F_{po} against $-\gamma_{lv}\cos\theta$ in Figure 3. This plot indicates that the work required to wet the methyl-terminated surfaces is greatest, producing the strongest adhesion between methyl-terminated surfaces. The more hydrophilic surfaces, as identified from their contact angles with water, show reduced adhesion. Since $F_{po} \propto w$, the curvature in this plot is attributed to variations in γ_{sv} for different chemical terminations. We can use this curvature to estimate values for γ_{sv} for the higher energy surfaces (OH-, CO_2H-, and $CO(NH_2)$-terminated monolayers). Using a simple graphical approach, for each data point (monolayer termination) we compare the observed pull-out force to that expected for a constant γ_{sv} (dashed line). The difference in the surface energy needed to place the observed measurement along the dashed line (the displacement along the abscissa labeled $\Delta\gamma_{sv}$) represents the increase in surface energy for that monolayer coating above the known value for the CH_3-terminated surface. Thus, to estimate γ_{sv} for the CO_2H-terminated surface, we add $\Delta\gamma_{sv} = 35$ mN/m to $\gamma_{sv} = 19.5$ mN/m, to obtain $\gamma_{sv} \geq 55$ mN/m. (The inequality results from our application of Young's equation at small contact angles.) Similarly, $\gamma_{sv} \geq 55$ mN/m for the $CO(NH_2)$-termination. For the OH-terminated surface, a smaller displacement of $\Delta\gamma_{sv} = 20$ mN/m corresponds to a smaller surface energy of $\gamma_{sv} \geq 40$ mN/m for the hydroxy-terminated surface. These estimates are consistent with recent estimates for γ_{sv} derived from interfacial force measurements in dry nitrogen.[22]

For tips and samples comprised of the same *bulk* solid material, γ_{ts} should be zero. The monolayers used in this set of measurements, although alike, are not bulk solids and thus γ_{ts} need not be zero. We can evaluate γ_{ts} from eq 1, by ratioing the measured F_{po} values and w obtained in two solvents and solving for γ_{ts}. We thus determine $\gamma_{ts} = 0.9\pm0.4$ mN/m for the methyl/methyl interface. Similarly, we determine $\gamma_{ts} = 0.3\pm0.8$ mN/m for the methoxy/methoxy interface.

The JKR model of adhesion mechanics[23] can be used to estimate the tip radius, R, and the effective contact radius, a_s. Within this model, the contact area under adhesion is given as

$$a_s = \left(\frac{3\pi R^2 W}{2K}\right)^{1/3}$$

where R is the radius of the tip at pull-off, W is the surface energy per unit area, and K is the elastic moduli of the monolayer-coated surfaces.[19] The pull-off force relates to the tip radius at pull off as

$$F_{po} = -\frac{3\pi}{2}RW$$

We thus estimate a tip radius of ≈300 Å from the 12.5 nN pull-out force and 92.7 mN/m work of adhesion per unit area of methyl-terminated surfaces in contact in water. From the elastic moduli of the gold surface, $K = 64$ GPa, the contact area is thus determined as $a_s \approx 10$ nm^2, or the equivalent of 50 contacting molecules under adhesion.

For measurements performed in water, the solvent exclusion effect (and the observed pull-out forces) are chemically intuitive: Water does not wet the hydrophobic methyl-terminated surfaces, and a large pull-out force is thus needed to break the tip−sample contact. Water easily wets the hydrophilic surfaces (hydroxy-, carboxy-, and amide-terminations), and much smaller pull-out forces suffice to break the tip−sample adhesion. With water as the solvent, the magnitude of this effect is substantial, and should serve as a means to enhance chemical contrast in imaging such chemically distinct surfaces.

The measurements in ethanol span a much narrower range. Nonetheless, we consistently observe a greater adhesion between

---

(22) Thomas, R. C.; Houston, J. E.; Crooks, R. M.; Kim, T.; Michalske, T. A. *J. Am. Chem. Soc.* **1995**, 117, 3839−3834.

(23) Johnson, K. L.; Kendall, K.; Roberts, A. D. *Proc. R. Soc. London, A* **1971**, 324, 301.

Table 4. Summary of Pull-Out Forces (nN) Recorded in Solvents between Samples and Cantilever Tips Covered with Different Self-Assembled Monolayer Coatings

alkanethiol coatings	Solvent	N[a]	force	σ_F[b]
$HS(CH_2)_{10}CH_2CH_3/HS(CH_2)_{10}CH_2OCH_3$	Water	4	5.82	2.71
	EtOH	4	0.86	0.46
	HD	6	0.32	0.15
$HS(CH_2)_{10}CH_2CH_3/HS(CH_2)_{10}CH_2OH$	Water	5	1.36	0.41
	EtOH	6	0.26	0.06
	HD	5	0.26	0.12
$HS(CH_2)_{10}CH_2OCH_3/HS(CH_2)_{10}CH_2OH$	Water	5	1.81	0.70
	EtOH	4	0.09	0.06
	HD	4	0.68	0.40

[a] Number of independent tip/sample combinations used in the determination. [b] σ_F denotes the standard deviation in the measurement of pull-out forces.

CH_3-terminated surfaces ($F_{po} = 2.3 \pm 1.1$ nN) than between the other surfaces (e.g. $F_{po} = 0.27 \pm 0.04$ nN for CO_2H-CO_2H contacts).[24] The low energy and relative wettability ($\theta_{EtOH} = 40°$) of the CH_3-terminated surface should give rise to a small pull-off force in ethanol. Consequently, exclusion of ethanol from the interface cannot entirely account for this adhesion. The explanation must lie in microscopic details. One possibility is that the order along the alkane thiol chain endings is solvent dependent. Greater fluidity at the chain endings would increase the opportunity for tip−sample interdigitation, generating greater adhesion between these alkane thiol coatings. The weaker adhesion between the CO_2H-terminated coatings would thus indicate less interdigitation between these monolayer coatings, as one would expect for hydrogen-bonding terminations. Finally, we note that because HD is a nonpolar low surface energy medium, it serves as an excellent lubricant for all chemical terminations that we have investigated. With such minimal adhesion, solvent exclusion cannot be an effective source of chemical contrast, making HD an ineffective medium for “chemical AFM”.

Chemically Distinct Samples and Tips. Adhesive force measurements performed on tips and samples with different terminal functional groups show similar solvent exclusion effects. A data set was generated from tips and samples covered with three different monolayer coatings: the methyl-terminated ($HS(CH_2)_{10}CH_2CH_3$), methoxy-terminated ($HS(CH_2)_{10}CH_2OCH_3$), and the hydroxy-terminated ($HS(CH_2)_{10}CH_2OH$) monolayers. The pull-out forces were then recorded between tips and samples, each covered with a different one of these monolayer coatings, and the results are summarized in Table 4. In general, the magnitude of the observed pull-out force is unchanged upon switching the tip and sample monolayer coating.

Inspection of Table 4 shows that the range of forces recorded in different solvents is greatest in water, smaller in ethanol, and smallest in *n*-hexadecane, following the trend which was observed between like tips and samples. For these interfaces between chemically distinct monolayer coatings, it is noteworthy that the greatest adhesion in water occurs for the most hydrophobic combination that we have studied (the methyl/methoxy interface), with an average pull-out force of 5.82 nN. This combination also shows the greatest adhesion in ethanol (0.86 nN). Recalling the smaller adhesion between like methoxy contacts in both water and ethanol, this result suggests that solvent effects, rather than specific chemical interactions between terminations, is more important for regulating adhesion between these monolayer surfaces. In other words, specific chemical interactions between terminal groups appear less significant than the work required to separate the tip−sample interface in the liquid media.

Applications

Having established the important contribution of solvent exclusion on the adhesion forces, we would like to exploit this effect to enhance chemical contrast in AFM imaging. One approach is to generate a “force volume” map of the surface, in which the pull-out force is recorded at each point on the surface.[25] Such data acquisition is relatively slow, however, and not readily done with all commercial microscopes. Alternatively, frictional (or lateral) force measurements (LFM) can be performed and the LFM signal (F_f) can be related to the pull-out force,[26]

$$F_f = \mu L + F_{po} \tag{4}$$

where L is the applied load and μ is the friction coefficient. Since μ scales with F_{po}, it follows that the variations in adhesive forces described above will convey to F_f, providing a chemical contrast in the LFM images. Equation 4 further indicates that the chemical contrast may be enhanced by increasing the applied load.

To explore the feasibility of this approach, we report initial findings for scanning force measurements on Pebax 1074, a segment copolymer consisting of polyethylene glycol and polyamide (Nylon-12) blocks in nearly equal proportion. Since this copolymer includes both hydrophilic (polyethylene glycol) and hydrophobic (polyamide) blocks, it is not water soluble but displays a relatively small macroscopic water contact angle of ∼40°. On the basis of the force measurements described above, we anticipate that in water a (moderately hydrophobic) methoxy-terminated tip will adhere most strongly to more hydrophobic regions of the polymer surface (exposed polyamide blocks) than to hydrophilic regions (exposed polyethylene glycol blocks), introducing contrast in the LFM images. The more hydrophilic amide-terminated tip should adhere more weakly in water to both hydrophobic and hydrophilic regions of the surface, yielding less contrast in LFM images. Figure 4 shows topographic and LFM images acquired in water with these two tip terminations. Note that the topographic images obtained in water (Figure 4a,c) are of comparable quality for both tip terminations. Differences in contrast become apparent in the lateral force images, which relate more directly to variations in adhesion. The methoxy-tip-generated LFM image (Figure 4b) displays additional friction absent in the amide-tip-generated LFM image (Figure 4d). As described above, we attribute this greater friction in the methoxy-tip-generated image to regions of the polymer surface which remain enriched with polyamide blocks. Because of the solvent exclusion effect, these regions will adhere most strongly to the methoxy-terminated tips, thus appearing with enhanced contrast. We generally expect (and observe) the amide tip to adhere more weakly to both the polyethylene glycol and polyamide blocks (Table 2), exhibiting less friction (contrast).

---

(24) The ordering of the adhesive forces that we observe reproducibly over a 2 year period in ethanol [F(CH_3-terminated surfaces) > F(CO_2H-terminated surfaces)] contradicts the results of Lieber *et. al.*[1,2] These differences likely reflect real chemical differences between these investigations. Lieber *et al.* may have utilized CO_2H-terminated monolayers with a different methylene chain length than the $(CH_2)_{10}$ chains employed in this study, leading to structural (and hydrogen-bonding) differences between the monolayer surfaces. These differences could also reflect different water content in the ethanol solvent.

(25) van der Werf, K. O.; Putman, C. A. J.; de Grooth, B. G.; Greve, J. *App. Phys. Lett.* **1994**, *65*, 1195−1197.

(26) Binggeli, M.; Mate, C. M. *J. Vac. Sci. Tech. B* **1995**, *13*, 1312−1315.

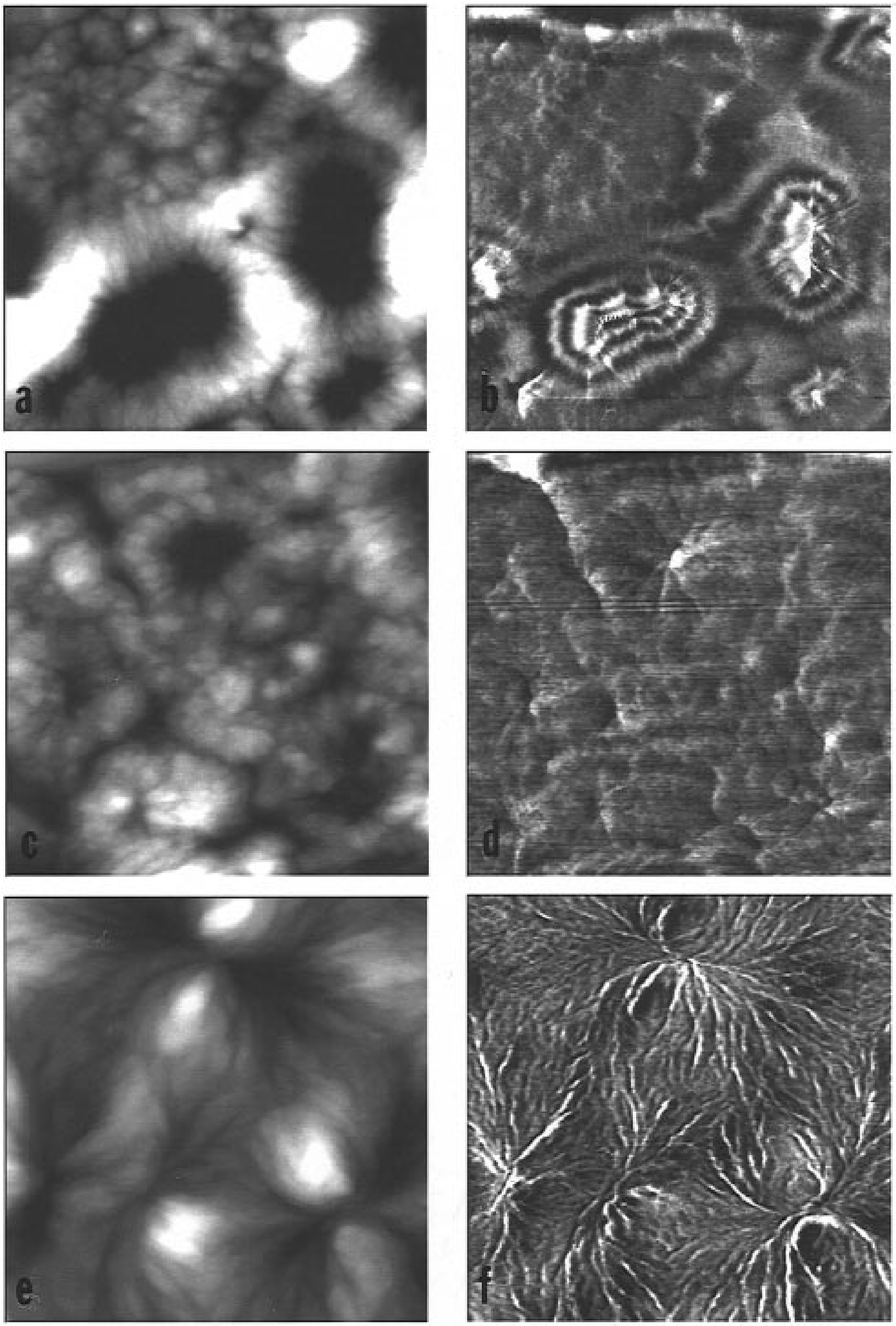

Figure 4. Solvent-exclusion contribution to image contrast is demonstrated with scanning force data acquired on a *co-block*-polyethylene glycol−polyamide (Nylon-12) surface (PEBAX 1074), prepared by melting/resolidification. (a) Topographic image in water, methoxy tip termination (15 μm x 15 μm); (b) LFM image in water, methoxy tip termination (15 μm x 15 μm); (c) topographic image in water, amide tip termination (7.5 μm x 7.5 μm); (d) LFM image in water, amide tip termination (7.5 μm x 7.5 μm); (e) topographic image in air, methoxy tip termination (4.5 μm x 4.5 μm); and (f) LFM image in air, methoxy tip termination (4.5 μm x 4.5 μm).

Finally, we emphasize that the chemical contrast introduced by solvent exclusion provides a useful complement to that obtained in air. By performing these measurements in air (Figure 4e,f), we eliminate the forces due to solvent exclusion, leaving the adhesion forces to be determined more directly by the tip−sample interactions. We find that LFM images acquired in air with both methoxy and amide terminations show strong lateral forces (friction). The magnitude of this friction is certainly increased by the strong (and uncontrolled) loading force due to the capillary action present in these “air” measurements. In fact, the strong adhesion between the polyamide tip and this polymer surface tends to smear resolution in the LFM images. Precisely because of its more moderate adhesion to the surface, the methoxy tip yields more richly detailed friction images in air (Figure4f, note prominent veins). The observed veins on the surface suggest orientational order of the polymer chains, which may be related to chemical composition. The extent to which this apparent orientational order is exaggerated by the mechanical compression of the polymer surface under loading forces is an open question. Much additional work is needed to sort out the mechanical, chemical, and “solvent-exclusion” contribution to force images acquired on such compliant surfaces. Experiments that incorporate chemically modified cantilever tips should prove helpful in addressing these issues.

Conclusion

The importance of the solvent in regulating adhesive interactions is critical to the interpretation of measurements performed in liquid media. We have demonstrated that solvent exclusion can directly affect the adhesive forces between cantilever tip and surface in scanning force measurements. This effect is most pronounced in water, in which the pull-out forces scale directly to the work due to solvent exclusion with the greatest adhesion between hydrophobic surfaces. In ethanol the adhesive forces are substantially smaller, but still sufficient to distinguish CH_3 surfaces from hydrophilic surfaces. In *n*-hexadecane the adhesive forces are negligible for all terminations. Solvent exclusion appears to dominate adhesion in water, but cannot simply account for forces recorded in ethanol, where solvent-mediated tip−sample interactions are suggested. This force data is used to evaluate the tip−sample interfacial energies (γ_{ts}) of like CH_3-terminated and ether-terminated surfaces, and the surface-vacuum interfacial energies (γ_{sv}) of the hydrophilic surfaces. Since solvent exclusion regulates adhesion between these model organic surfaces, it presents a source of chemical contrast in force imaging. We have tested this source of chemical contrast with friction force measurements of *co-block*-polyethylene glycol−polyamide polymer surfaces in water, obtaining chemical information that is complementary to that available in air images.

Acknowledgment. This research has been supported through NSF grants CHE-9417357 and CHE-9393962. Portions of this work were also supported by a Sloan Foundation Fellowship and a Packard Foundation Fellowship (J.E.R.R.). The authors would like to express their gratitude to Dr. S. K. Mirle and Dr. J. B. Lynch of W. R. Grace and Co. for many useful discussions and for providing the polymer samples.

JA961295C